IEEE Access
Multidisciplinary | Rapid Review | Open Access Journal

Received September 7, 2018, accepted November 29, 2018, date of publication December 5, 2018,
date of current version December 31, 2018.

Digital Object Identifier 10.1109/ACCESS.2018.2884922

Novel Approach for Three-Dimensional Integral Documentation of Machine Rooms in Hospitals Using Portable Mobile Mapping System

MANUEL RODRÍGUEZ-MARTÍN[1,2], PABLO RODRÍGUEZ-GONZÁLVEZ[3], DIEGO GONZÁLEZ-AGUILERA[1], AND ERICA NOCERINO[4,5]

[1]TIDOP Research Group, Polytechnic School of Avila, University of Salamanca, 05003 Ávila, Spain
[2]Technological Department, Catholic University of Avila, 05005 Ávila, Spain
[3]Department of Mining Technology, Topography and Structures, Universidad de León at Ponferrada, 24401 Ponferrada, Spain
[4]Laboratoire des Sciences de l'Information et des Systèmes, Aix-Marseille Université, 13007 Marseille, France
[5]Theoretical Physics, ETH Zürich, 8092 Zürich, Switzerland

Corresponding author: Manuel Rodríguez-Martín (ingmanuel@usal.es)

ABSTRACT In this paper, a novel method for the documentation and evaluation of the machine rooms in hospitals is presented. The approach is based on data acquired with a portable mobile mapping system (PMMS), GeoSlam Zeb-Revo, which has proved to be effective for three-dimensional (3D) mapping of indoor environments, as well as for 3D modeling of individual thermal and fluid-mechanics equipment. An automatic data processing workflow based on the extraction of quantitative and qualitative geometrical features from the point clouds provided by the PMMS is developed with the aim of evaluating the state and adequate distributions of machineries and, in this way, generating a complete three-dimensional map of the industrial environment to be used for maintenance, inspection, and inventory tasks in accordance with safety standards. The extracted parameters are statistically tested to evaluate the adequacy of the proposed methodology and, in this way, demonstrate its potential for the application in the context of hospital facilities.

INDEX TERMS Maintenance engineering, optical sensors, statistical analysis, portable mobile mapping system, handheld, 3D processing, hospital facilities.

I. INTRODUCTION

Geomatic techniques, sometimes referred as geotechnologies, include a range of sensors and algorithms aiming at the acquisition, modelling and analysis of spatial features [1]. As result, they are suitable to highlight and quantify changes in space and time. Geomatics techniques are commonly employed to obtain 3D models for documentation purposes and can be successfully applied also for industrial and energy applications. As examples of reverse engineering, in [2] terrestrial laser scanner was applied for the reconstruction of electrical substations; the obtained point clouds are used as base for CAD design of the different discrete elements. In [3] and [4] another three-dimensional reconstruction of welded junctions from macro-photogrammetric point clouds and articulated coordinate machine were presented. The reconstruction from point clouds of complex industrial scenarios, as a nuclear power generation plant, has been also addressed by [5].

Mobile mapping systems (MMSs) are devices designed to obtain dense and geo-referenced three-dimensional point clouds of an environment while moving in it. These systems have been continuously improved since 1980s in term of density of the cloud, accuracy and acquisition time [6]. Their main potentialities are related with the reconstruction of objects of interest, as building, cultural heritage elements, civil structures and, also, industrial environments [7], and recently also for indoor environments [8]. Since there is no established nomenclature, and to distinguish them from vehicle-based MMS, authors will follow the term Portable Mobile Mapping System (PMMS) proposed by [6]. Although PMMS presents many similarities with classic MMS [9], nowadays these are the most innovative technique for surveying tasks [7].

PMMS are equipped with navigation and remote sensing modules. The navigation module usually consists of an Inertial Measurement Unit (IMU) and, sometimes, also a Global Navigation Satellite System (GNSS) receiver/antenna; the remote sensing module normally features laser scanning sensors and, sometimes, also different types of cameras (spherical, panoramic, wide-angle or standard). A deep review about

this emerging technology, the different typologies of PMMS and comparison among them and their applications is presented in [6].

Among the different types of PMMS, including backpacks and trolleys, handheld PMMS are the most popular the GeoSLAM Zeb-Revo, in spite of its novelty, has already been employed for different uses related with civil engineering [10], [11], cultural heritage documentation [12], disaster analysis [13] and forestry engineering [14]. Its main characteristics are the lack of GNSS, and the use of a 2D laser to reconstruct different environments. Currently the number of application areas of handheld PMMS devices is still growing. In [15],the GeoSLAM Zeb-Revo and Leica Pegasus:Backpack are compared on the basis of a robust statistical assessment. The results stated that both PMMS performed within vendors specification, but with the GeoSLAM Zeb-Revo generally outperforming the declared values despite the present of evident gross errors in the outdoor scenario. These results in conjunction with the lower acquisition cost of the handheld, justify the chosen of the GeoSLAM Zeb-Revo for the presented research, to explore the potentialities of this device within the industrial context, i.e. thermal facilities. Moreover, its relative affordable cost improves its competitiveness form the point of view of the final users, usually stakeholders and/or maintenance companies.

On the other hand, the machine rooms of hospital complex require a rigorous control and a constant monitoring to assure that nothing fails. Hospitals are really singular facilities which have to be designed under higher safety requirements and the production and storage capacity, both hot water, oxygen, steam, compressed air and other substances must be oversized to ensure supply in case of failure. Moreover, rigorous periodic maintenance programs with complexes inventories of the different equipment, pipes, valves and other auxiliary elements are required. That is the reason machine rooms of the hospitals represent a complex industrial context normally physically separated from the hospital, in their own constructions (although, connected to them).

Distribution of boilers and other thermal equipment within the machine rooms are indicated by the standards, in this way, meeting geometric requirements in the distribution is mandatory (e.g. distance among boilers, geometric and volumetric conditions of the room, etc.) following the different national standards (e.g. currently applicable standards in Spain are [16], [17]). For this reason, the generation of a three-dimensional recording of the rooms with PMMS is highly useful in order to ensure the quality of the service and supply and ensure and, even, consider possible maintenance, expansion and improvement actions based on accurate, scaled and documented geospatial information (point clouds), traceable, which can be consulted at any time. Then, over the point clouds model, different algorithms will be applied for the remote estimation of geometrical features as diameters of pipes, diameters of homes, misalignments and distance between equipment. Using these parameters, statistical methods will be applied for the automatic detection of defects and maintenance tasks in the equipment in order to assess the suitability of state-of-the-art PMMS as the GeoSLAM Zeb-Revo.

II. CONTEXT

This research is carried out in the machine room of a European medium size hospital (around 500 beds). The machine room of the hospital has the following equipment (Table 1) in a diaphanous attached industrial building (450 m^2) with different access for maintenance tasks.

TABLE 1. Numbering and definition of the main equipment of the machine room.

Equipment	Number	Thermal and fluid-mechanics parameters of the equip
Industrial steam boilers	2	Head power: 1163 kW Steam production: 1725 kg/h Max. service pressure: 11,7 bar
Heating boilers	4	Head Power: 1110 kW Max. service pressure: 10,0 bar
Head water tanks	3	Volume storage: 8000 l Max. service pressure: 8,0 bar
Other equipment		• 1 head water boiler • 2 compressors • 2 compressed air tanks • 1 compressed air tank • Decalcification equipment • Plate head exchangers • Auxiliary water pumps • Water pipes • Steam pipes • Compressed air pipes • Smoke evacuation system • Fans

III. MATERIALS AND METHODS

A. MATERIALS

The commercial PMMS used for this research is Zeb-Revo [18], from the company GeoSLAM. It is the evolution of the first version, ZEBedee, developed by the Autonomous Systems Laboratory, CSIRO ICT Centre in Brisbane (Australia) [19], which consisted on a 2D profilometer moved with an elastic support. The Zeb-Revo is equipped with an IMU as navigation module and a 2D profilometer (UTM-30LX), which is continuously rotating during the data acquisition. Then, the device has also an integrated commercial camera Go-Pro hero installed in order to record the scenario during the reconstruction and, in this way, any element can be also located on image. The 2D laser profilometer is a compact laser scanning range finder, which consume less power, is more compact and light-weight than a classic 3D laser scanner system [15].

The navigation module is constituted by an IMU, placed close to the 2D profilometer to control the position during the rotation movement of the sensor and also during the displacement of the operator. Due to the rotation, the system records three-dimensions information of the scenario, allowing the application of the 3D-SLAM. The data are controlled and

TABLE 2. Key technical features of the Zeb-REVO PMMS.

Technical features	
Measurement range (indoors environment)	30 m
Measurement range (outdoors environment)	15 m
Data capture speed	43200 points/s
Accuracy	±0.1%
Field of view	360 º (V) x 270 º (H)

stored on a server with a hard disk located the backpack, which is part of the system and that is carried on the back by the operator. Specific features of the Zeb-REVO are shown in Table 2.

B. METHODS

The developed methodology is outlined in Fig. 1 and it focuses on the extraction of qualitative information and quantitative parameters of the machine room from the point clouds generated by the PMMS following the indicated steps described in the next subsections.

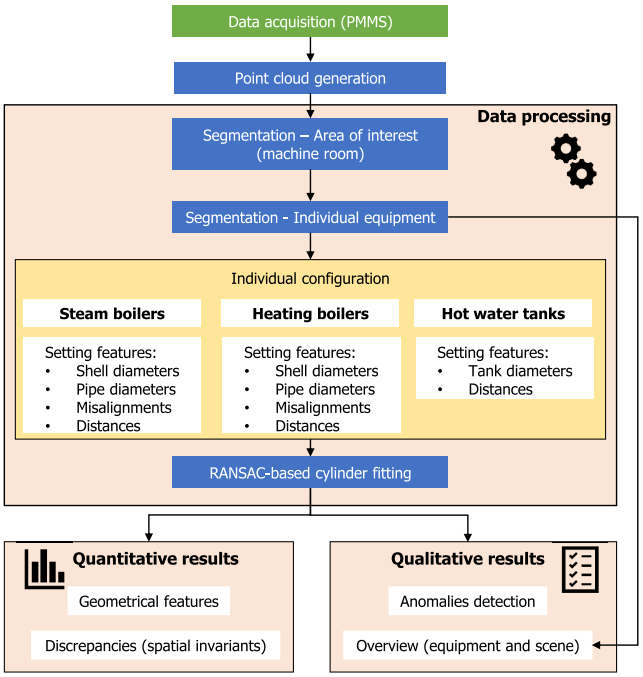

FIGURE 1. Methodology followed to obtain the qualitative and quantitative results.

1) DATA ACQUISITION PROTOCOL AND POINT CLOUD GENERATION

One of the most important peculiarities of non-GNSS PMMS is that to get the optimal results inspections should start and finish in the same position, so that the trajectory features a closed loop. In this way, the trajectory must be established so that the entire surface of the room or build are covered. The maximum acquisition time indicated by manufacturer is around 20 minutes in continuous mode, after which the quality of the provided results may be reduced, in this way, the trajectory must not be greater in length than the distance travelled by the operator at a slow pace during that time. However, this time requirement is sufficient to reconstruct large machine rooms with a single loop.

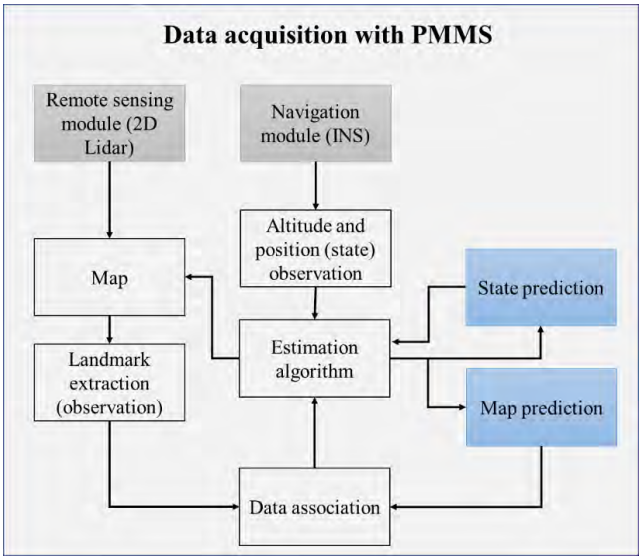

FIGURE 2. Process for data acquisition using ZEB-Revo device adapted from [6].

For a given time, both the sensor path and the map (i.e. position of geometric features or landmarks) are estimated at the same time without any prior knowledge. The navigation module provides clues for estimating the system position and attitude, while the remote sensing module generates the data to build the map from where the landmarks are extracted. The problem of navigation and mapping is automated and partly or even entirely based on the so called simultaneous localization and mapping (SLAM) algorithms, as it is indicated in Fig. 2. This is a recursive and sequential two-step approach. A prediction of the time-updated system location and map is produced according to the navigation module input and the past trajectory and dynamics. The location and map predictions are confronted to and corrected with the updated measurements (observations) derived from the navigation and remote sensing modules. For additional details about please refer to [6]. This operation is automated and carried out after data acquisition. The time needed for the processing is related to the trajectory length and scene complexity.

After the data collection and processing, the point cloud is generated in a local coordinate reference system. It can be georeferenced in a geographic reference system by means of rigid Helmert transformation if control points are visible in the acquired data. Alternatively, the individual points clouds can be reference in the same local system by means an iterative closest point (ICP) registration [20].

2) DATA PROCESSING

The obtained point clouds can be visualised in a proprietary viewer (GeoSlam Viewer) that allows also to show the images

from the video caption of attached camera over the trajectory. However, the mere visualization of the point cloud in its raw state is not the object of this study, but rather it is intended as input to extract parameters of industrial interest from the machine room. The PMMS point clouds are processed in an GPL software CloudCompare v2.9.1 [21]. Initially designed for comparison between dense 3D points clouds, it has been extended to provide advanced algorithms and plugins for point cloud processing, as registration, resampling, interactive or automatic segmentation…The software is used for the segmentation of the point cloud in order to extract the parts of interest, discarding those that have no interest in the evaluation of equipment (ceilings, beams, walls, pipes, obstacles, etc.). This process is manually implemented with the selection and segmentation tools provided by the software. Moreover, the comparison algorithms will be employed between the acquired geometry (as point cloud) and the theoretical (as mesh). The theorical surface is obtained from the RANSAC-based cylinder fitting.

Once the area of interest is extracted, the distribution of the equipment in the room is an important result, for maintenance works, evaluation of compliance with standards, or for expansion or engineering work within the room.

The next step is the manual segmentation of the individuals point clouds referring each of the equipment (boilers and tanks). This is also implemented using the selection and segmentation tools of the CloudCompare software [21]. The individual segmentation of the equipment allows the possibility of differentiating them with colours to obtain a three-dimensional overview of the distribution of the machine room with the different equipment properly segmented. It is possible to take measures directly on the point clouds because the information given by the sensor is scaled.

In addition to the distribution, specific information about the different parameters of the equipment must be extracted. In this case, different procedures are applied for the extraction of different significant characteristics for each type of machine (Table 3), according to mathematical criteria that avoid the uncertainty of manual measurement over the point clouds.

As the reader can see, the most important characteristic can be defined in function of three typologies of geometrical parameters: diameters, distances and angles as descriptive characteristics which come from the cylinder fitting processing. It will be explained in the next paragraphs.

Diameters are important parameters to define and study pipes, shells of boilers and tanks. All of them are important elements in the machine rooms. The diameter of an object is extracted from the individual point cloud for each equip. For this aim, a processing based on a RANSAC Cylinder Filtering is applied [22]. This algorithm decomposes the point cloud into a structure based on inherent forms and a set of remaining points. Each detected form is used as a proxy for a set the corresponding points. This method is based on random sampling and can be used to detect different idealized geometries

TABLE 3. Numbering and definition of the quantitative parameters contemplated for the study of each characteristic of each type of equip.

Parameter	Description	Equipment	Descriptive characteristic
P_{1i}	Smoke evacuation pipe	Steam boiler (SB)	Diameter
P_{2i}	Steam outlet pipe		
$P_{3a\,i}$	Pipe for safety valve		
$P_{3b\,i}$	Pipe for safety valve		
$P_{gas\,i}$	Gas inlet pipe		
$D_{SB\,i}$	Shell diameter		
δ_i	Shell misalignment		Misalignment
$d_{SB\,j}$	Distance between equipment		Distance
P_{1i}	Smoke evacuation pipe	Heating boiler (HB)	Diameter
P_{2i}	Heating water outlet pipe		
P_{3i}	Pipe for safety valve		
$P_{gas\,i}$	Gas inlet pipe		
$D_{HB\,i}$	Shell diameter		
δ_i	Shell misalignment		Misalignment
$d_{HB\,j}$	Distance between equipment		Distance
$D_{T\,i}$	Tank diameter	Tank (T)	Diameter
$d_{T\,j}$	Distance between equipment		Distance

in point clouds models, as planes, spheres, cylinders, cones and tore. In this case the algorithm is used to detect and fit cylinders.

Firstly, a sample of the points of a tubular geometry are extracted using the selection and segmentation tools provided by CloudCompare. Over these specific points which really represent the surface of the cylinder, RANSAC algorithm is applied to fit a cylinder, which is defined by a diameter, a length and a position (centres of initial and finish circumference). The standard deviation of each point in relation to the fitted cylinder are evaluated to obtain statistical information that can be used to analyse the quality of the adjustment and to detect anomalies in the histogram that could constitute an anomaly that should be studied individually as will be explained in the next subsection. The cylinder fitting based on RANSAC algorithms are also the base for the extraction of the next parameters.

Once a cylinder fitting procedure based on RANSAC algorithm has been applied, the extraction of the edge for each cylinder i is possible if the edge is defined as a vector $(\boldsymbol{E_i^x}, \boldsymbol{E_i^y}, \boldsymbol{E_i^z})$. The angle $\boldsymbol{\delta_i}$ between this vector and the ground is calculated with definition of scalar product (1).

$$\boldsymbol{\delta_i = atg}\left(\frac{\boldsymbol{E_i^z}}{\sqrt{(\boldsymbol{E_i^x})^2 + (\boldsymbol{E_i^y})^2}}\right) \tag{1}$$

Misalignment is useful for the accurate study of the location of each equip within the machine room and, also, to estimate some aspects related to the drainage of water condensations into the equipment and/or pipes.

Distances among equipment are critical parameters for the security and operability study of the machine rooms. The standards usually establish the specific requirements about distances between boilers, tanks and other equipment to ensure the security and the correct access for maintenance and conservation. These distances are not an easy parameter to measure with great accuracy because not always the equipment is arranged in a totally parallel way. In this way, the distance is estimated from the point cloud based on the separation of the fitted cylinders associated to the shells of the boilers and tanks. Each shell of the steam boilers, heating boilers and tanks presents a concrete diameter.

The procedure to estimate the distance between boilers is based on the extraction of the fitted cylinder for each shell being i the number of the equipment and $\boldsymbol{j = i-1}$ the number of the distances between equipment. After, the Euclidian distance two to two from the centre of the four bases of cylinders is calculated. In this way, two distances are generated ($\boldsymbol{L_{j1}}, \boldsymbol{L_{j2}}$) and the smallest ($\boldsymbol{L_j}$) is chosen to assess the more critical situation with respect the standards (2). If the distance Lj verifies the minimum safety distance according to the standards, then the equipment arrangement is verified. The distance is calculated (3) subtracting the shells radius $\left(\frac{\boldsymbol{D_i}}{\boldsymbol{2}}, \frac{\boldsymbol{D_{i+1}}}{\boldsymbol{2}}\right)$ in order to obtain the minimum distance between equipment $\boldsymbol{d_j}$.

$$L_j = \min\{L_{j1}, L_{j2}\} \tag{2}$$

$$d_j = L_j - \left(\frac{D_i + D_{i+1}}{2}\right) \tag{3}$$

3) DISCREPANCIES AND ANOMALIES DETECTION

The cylinder fitting is a procedure to fit the three-dimensional distribution of points. The deviation between the position of each point and the idealized fitted cylinder allow to quantify spatially the precision of the fitting and/or to detect outliers. These last one could be caused by measurement errors, such us flying points, or SLAM reconstruction errors; or by the fact that the studied object does not fulfil the initial hypothesis (complete cylindrical shape). This calculation is carried out between the acquired point cloud and the fitted cylinder in form of a mesh. The discrepancies can be analysed in absolute terms or, however, in relative terms (deviation of the diameter by diameter unit). It should be noted that if this distribution does not present outliers, it can be considered as a representation of the noise.

The normality of the data derived from sensors such as laser scanners cannot be assured a-priory [23]. In the sample size, if higher, as alternative to normality tests, the Gaussian assumption has to be assessed visually. Both reported tests are the histogram of the signed differences with the superimposed curve for the normal distribution, and the quantile-quantile (Q-Q) plot of the distribution of the signed differences [15]. The deviation from the theoretical shape (bell and/or straight line) indicate a non-normality, either by the PMMS or the studied object.

These statistical results are useful to evaluate the quality of the applied approach. In this way, higher relative values for the deviation results can be interpreted as a low level of precision. However, small values for relative deviation ensure the quality of the model and validating, in this way, the initial hypothesis. Nevertheless, the statistical results provide an additional application since the computation of distances between the fitted cylinders and points could be the basis for the automatic detection of surface defects in pipes and shells and, also, for the automatic detection of maintenance tasks in the different equipment based on anomalies of the histogram.

IV. RESULTS

As it was indicated in Fig. 1, the results of the present research are classified in two categories. On the one hand, qualitative results and, on the other hand, quantitative results. First are formed by the overview and anomalies detection, while the second are formed by the geometrical features and discrepancies. Next, the results will be displayed in order of obtaining them within the process.

A. OVERVIEW (EQUIPMENT AND SCENE)

The goal is to provide a general record of the scenario. The segmentation allows to apply a semantic labelling of the different elements, and its subsequent application to the optimization of environments, risk management (prevention and identification of risks). It also forms a 3D snapshot of the state of the scenario and all the contained elements that allow a study of the life cycle of the installation, being these qualitative results useful in itself for the indicated tasks.

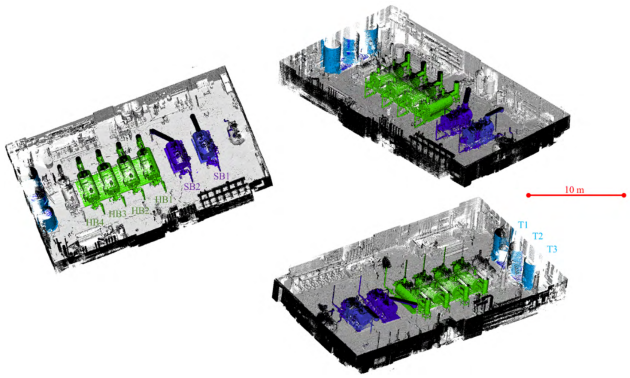

FIGURE 3. Overview results: 3D map of the machine room, and segmentation of the different equipment (purple: steam boilers, green: heating boilers, blue: hot water tanks).

Following the methodology up to what is established in the subsection III-B-2), a global three-dimensional model which the global stage is generated (Fig. 3) and the trajectory followed by the operator (Fig.4) for the data capturing is indicated, being the time spent in this of 250 seconds for the scene stated in section II. Please note that the trajectory shown

TABLE 4. Parameters of steam boilers obtained by PMMS (units in m, except Δ in degrees).

Parameter	SB1		SB2	
	Mean diameter	Std. dev	Mean diameter	Std. dev
D	1.604	± 0.009	1.608	± 0.007
P_1	0.529	± 0.012	0.526	± 0.010
P_2	0.182	± 0.019	0.178	± 0.020
P_{3a}	0.122	± 0.018	0.120	± 0.009
P_{3b}	0.119	± 0.012	0.122	± 0.010
P_{GAS}	0.078	± 0.008	0.077	± 0.007
d	1.716			
δ	-0.7564		0.6361	

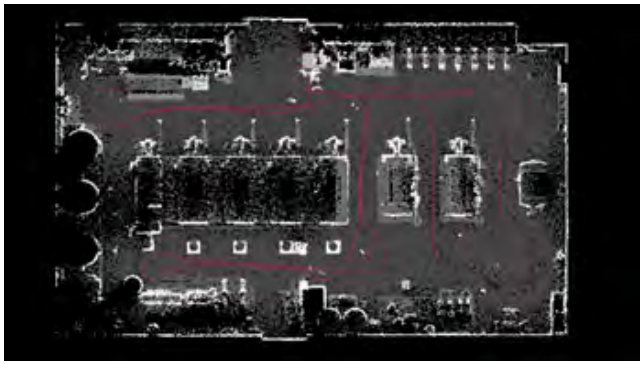

FIGURE 4. Followed trajectory over the plant view for the data acquisitions using Zeb-Revo.

in Fig. 4 is was constrained near the hot water tanks by the presence of obstacles. However, this fact did not affect the final results.

From the global scene each equip is segmented, obtaining individual point clouds for each of them, as it is shown in Fig. 4. with different colours.

B. QUANTITATIVE PARAMETERS OF THE EQUIPMENT

Once, the 3D map has been obtained and the equipment has been segmented (Fig.3), the methodology described in subsection II-B-2) is applied to the individual point clouds of the equipment in order to extract the quantitative parameters for each of them (Table 3). Firstly, we addressed the steam boiler, after, the heating boilers and, finally, the hot water tanks. In order of higher to lower complexity.

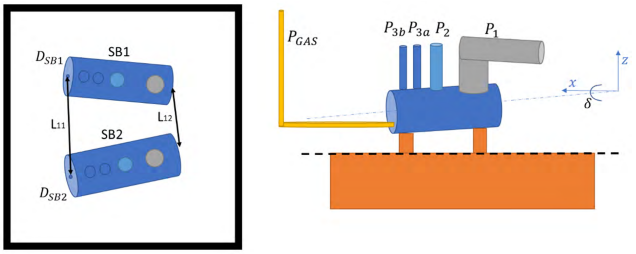

FIGURE 5. Individual quantitative parameters extracted following the process for the steam boilers. Left: Elevation view of the equip. Right: front view of the equip.

1) STEAM BOILER

The parameters established in Table 3 for the steam boilers (Fig. 5) are extracted following the proposed methodology. In this way, diameters, angles (Eq. 1) and distances (Eq. 2, 3) are estimated from the fitted cylinder. Also, the standard deviation of the cylinder adjustment is shown in Table 4.

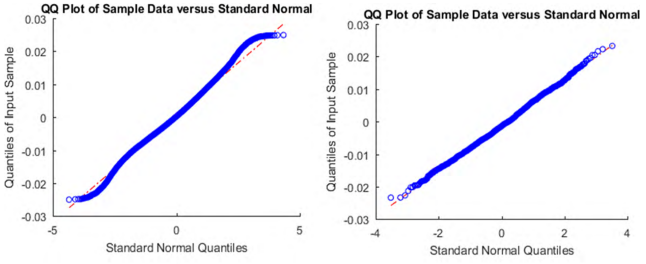

FIGURE 6. QQ-plot of SB2 shell diameter (a) and gas inlet pipe (b) parametric fitting error.

The statistical parameters selected for Table 4 were the Gaussian estimator for error central tendency (mean) and dispersion (standard deviation). The visual analysis by a QQ-plot shown that the follow an approximate Gaussian distribution as shown in Fig. 6 for the two more significant and extreme parameters: the largest (shell diameter) and smallest (gas inlet pipe diameter). This behavior is also supported by the histograms of fitting error (Fig. 7). This behavior is common for all parameters based on diameter characteristic for the steam boilers.

2) HEATING BOILERS

The parameters established in Table 3 for the heating boiler (Fig. 8) are extracted following the same methodology as previous. In Table 5 are shown the diverse diameters, angles and distances from the cylinder detection and fitting. As in the previous subsection, the statistical distribution of values is also supported by the histograms of fitting error for the shell diameter and the gas inlet pipe diameter (larger and smaller diameter respectively, just like the steam boilers).

As the reader can observe, all distributions have a Gaussian-like shape, expect the HB1 (Fig. 9a), which shows a significant asymmetry. This could have been caused by measurement error, or the non-fulfilment of the cylindrical hypothesis, e.g.: a deformation in the geometry due to an impact (this surface imperfection will be detailed in the subsection IV-C). The rest of the heating boilers show the good approximation to a Gaussian distribution.

TABLE 5. Parameters of heating boilers obtained by PMMS (units in m, except Δ in degrees).

Parameter	HB1		HB2		**HB3**		**HB4**	
	Mean	Std. dev	Mean	Std. dev	Mean	Std. dev	Mean	Std. dev
D	1.607	± 0.009	1.605	± 0.011	1.603	± 0.016	1.605	± 0.009
P_1	0.547	± 0.011	0.537	± 0.010	0.541	± 0.010	0.548	± 0.009
P_2	0.291	± 0.011	0.290	± 0.014	0.290	± 0.013	0.287	± 0.013
P_3	0.298	± 0.021	0.294	± 0.014	0.290	± 0.014	0.291	± 0.016
P_{GAS}	0.097	± 0.008	0.094	± 0.008	0.093	± 0.007	0.088	± 0.007
d	1.067		0.8834		0.884			
δ	0.4756		0.5386		0.7679		0.5214	

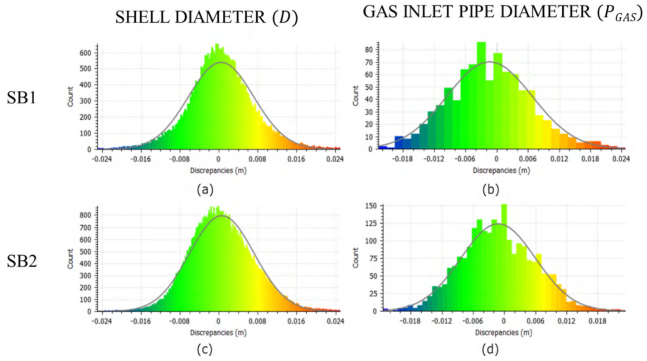

FIGURE 7. Histogram of parametric fitting of home boiler diameter for SB1 (a) and SB2 (c), and gas pipe diameter for SB1 (b) and SB2 (d). All the discrepancies are in meters.

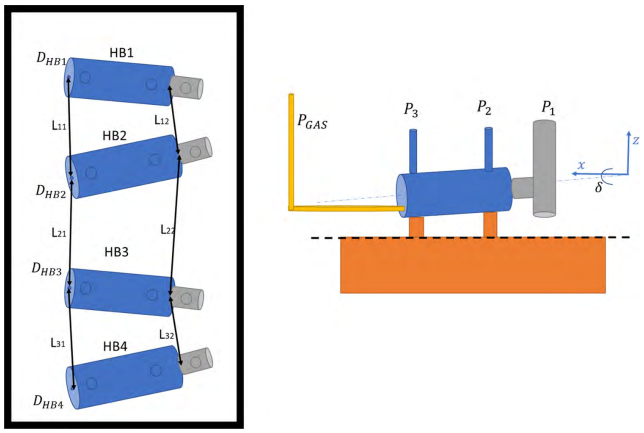

FIGURE 8. Individual quantitative parameters extracted following the process for the heating boilers. Left: Elevation view of the equip. Right: front view of the equip.

3) HOT WATER TANKS

Because of the geometrical simplicity of these devices, only two parameters have been extracted (Fig. 10): the tank diameter and the distance between tanks (Table 6).

The standard deviations of the diameters are shown in Fig. 11. As the reader can observe, the distribution for T1 and T3 are clearly approximated to a Gaussian distribution, but the distribution of T2 present peculiarities and a clear asymmetry provoked by a set of values far from the main tendency to the left side of the graphic (negative discrepancies). As for the heating boiler (HB1), it was found

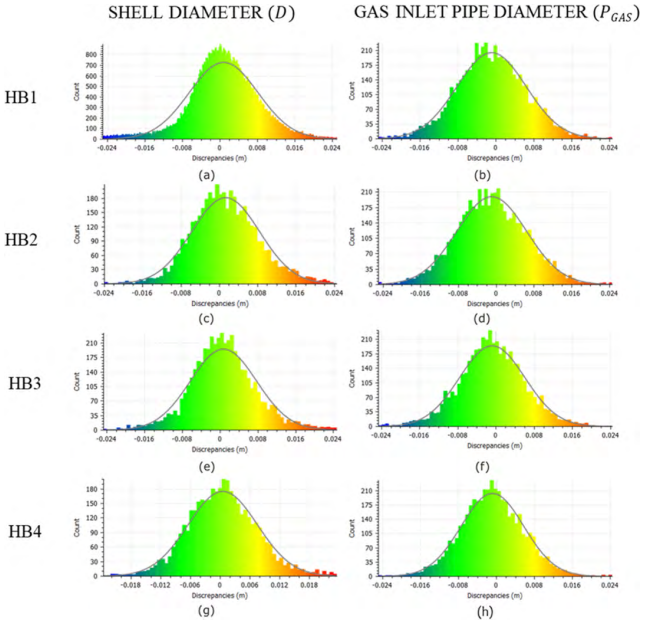

FIGURE 9. Histogram of parametric fitting of shell diameter for HB1 (a), HB2 (c), HB3 (e), HB4 (g), and gas pipe diameter for HB1 (b), HB2 (d), HB3 (f), HB4 (h). All the discrepancies are in meters.

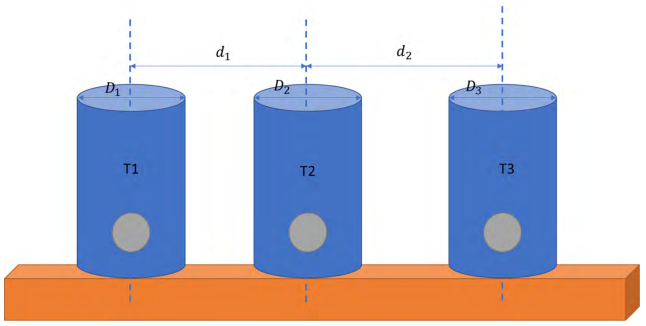

FIGURE 10. Individual quantitative parameters extracted following the process for the hot water tanks.

that the deposit had a surface anomaly because a plate of its shell was extracted for maintenance tasks and the isolation material of the deposit was on air, causing a decrease of the diameter in that area. This region was clearly identifiable, which is why it was segmented to analyze the trend (T2*), discriminating the effects of that area as it shown in Table 6.

TABLE 6. Parameters of the hot water tanks obtained by PMMS (units in m, except Δ in degrees).

Parameter	T1		T2		T3	
	Mean	Std. dev	Mean	Std. dev	Mean	Std. dev
D	1.819	± 0.011	1.832 1.839*	± 0.031 ± 0.020*	1.783	± 0.012
d	0.909		1.000			

* Values obtained after manual removal of the affected area.

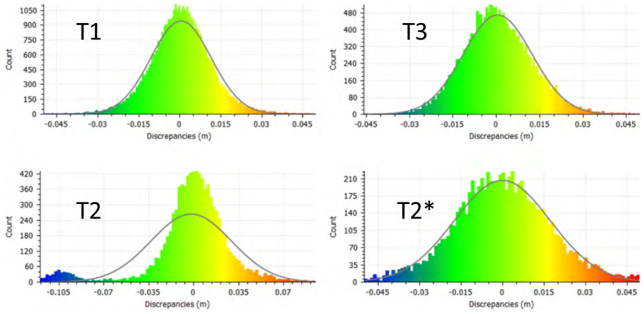

FIGURE 11. Histogram of parametric fitting of tank diameter for T1, T2 and T3. All the discrepancies are in meters. It is shown the original T2 fitting error, and the fitting error after the manual segmentation to exclude the area under maintenance (T2*). Please note the different X-axis scale in figure for T2.

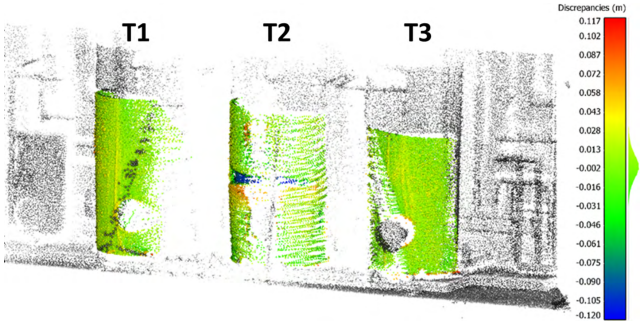

FIGURE 13. Point cloud referring to hot water tanks with the distances computed with respect the fitting cylinder for each of them. Please note the different in T2 (blue) where part of the shell has been removed for maintenance tasks.

C. ANOMALIES DETECTION

As the reader can see, results provided by the data processing allow the estimation of diameters with a standard deviation for each cylinder fitted. The presence of geometric anomalies on the surface reduces the credibility of the deviation values provided. In this way, the two anomalies detected during the date processing are independently studied to extract the depth map of the deformation zone for documentation tasks.

The HB1 presents a slight deformation located in the shell (compatible with a possible impact) that can be visualized in the point cloud after, establishing a distance computing between fitted cylinder and points to obtain a depth map of the zone. This anomaly has yet been suspected over the histogram (Fig. 9a). In the Fig. 12, the reader can appreciate a maximum radial deformation about 5 cm into the shell. There will be also possible to segment the anomalous area and quantify additional parameters such as affected area.

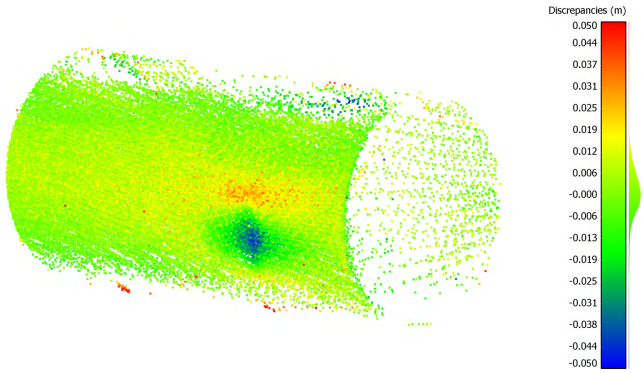

FIGURE 12. Slight deformation of the shell for HB1 (blue zone).

The T1 present a specific area with decrease in diameter due to the elimination of a part of the casing for maintenance work as it has been raised in the visual analysis of the histogram (Fig. 11). It is clearly visible in the point cloud where the discrepancy computation is shown for each point (Fig. 13). In this form, the blue zone, indicate the minimum diameter (maximum deformation of 12 cm towards the interior of the material).

D. DISCREPANCIES

The summary of the statistical parameters is completed by the standard deviation (SD) for all diameter values (Tables 4, 5 and 6). The individual SD values are averaged and normalized for each type of parameter of each machinery. As result is obtained the relative standard deviation (SDrel), which represents the ratio between the deviation and the mean of diameter for each evaluated parameter. The computation of the SDrel for each parameter is shown in Table 7. SDrel provides information about the impact of noise as percentage of the absolute value of the diameter, being most of points located within this range (± SDrel) with respect the main value of the diameter. Thus, it gives a more accurate idea of the deviation of the data with respect to the model generated in relative terms.

For further deepening, the SDrel-diameter data pairs for each parameter analysed are plotted as a 2D point cloud (Fig. 14) to study the correlation of the relative deviation of the points with respect to the diameter value for the different size of diameters. Different fitting methods are applied to study the possible existence of a dependence between the size of the diameter and the amplitude of the noise with respect the diameter (SDrel), being the more adequate the employment of an exponential fit by means of a robust estimation based on least absolute residuals (LAR) technique.

TABLE 7. Average discrepancies for each parameter.

Parameter	Mean (Av)	SDrel (Av)	Mean (Av)	SDrel (Av)	Mean(Av)	SDrel (Av)
	Steam boilers		Heating boilers		Hot water tanks	
D	1.606	± 0.50%	1.605	± 1.04%	1.835*	± 0.78%
P_1	0.527	± 2.07%	0.543	± 1.83%	-	-
P_2	0.180	± 10.72%	0.290	± 4.29%	-	-
P_{3a}	0.121	± 11.21%	0.293	± 4.78%	-	-
P_{3b}	0.121	± 8.96%			-	-
P_{GAS}	0.078	± 10.10%	0.093	± 11.09%	-	-

* Values obtained after manual removal of the affected by maintenance task area of T2.

TABLE 8. Statistical indicators of the exponential fit.

Fit type	a	b	c	SSE	R^2	RMSE
$ae^{-bx}+c$	16.08	4.786	0.7765	6.296	0.971	0.864

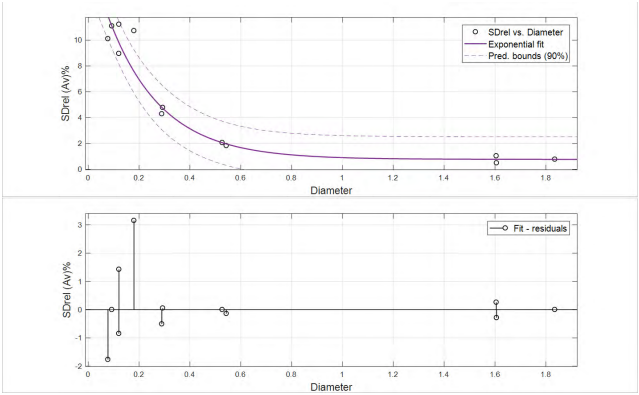

FIGURE 14. Up: Exponential fit of the mean value of the diameter with respect the relative standard deviation. Down: Fit residuals graph for each point.

Adjustment results show a clear trend of exponential decrease of the *SDrel* when the values of diameter grow, showing that the amplitude of the noise depends on the length of the diameter. This statistical conclusion is supported by very favorable error indicators, RMSE and R2 (Table 8), and is supported by the confidence bounds, as the reader can visualize in Fig. 14.

V. CONCLUSIONS

The present research provides a methodology based on a novel portable sensor for 3D mapping of industrial environments. GeoSLAM Zeb-Revo was chosen due to its high performance, operability, ease of use, data acquisition speed and good value for money. The data acquired with the system in machine rooms in a hospital allows the extraction of important features, such as conservation state and distribution. These features have been extracted based on three fundamental characteristics: distances, angles and diameters obtained from the point clouds.

Qualitative results allow a complete characterization of the environment. The overview allows an easy visualization of the whole of the room and its equipment, which in turn allows an individualization of the equipment and it is itself an important goal for the inventory and maintenance task of the machine rooms in order to guarantee the supply and security.

Once the individual segmentation is applied to each machinery, qualitative information can be extracted from the statistical distribution of the points, using a strategy based of histogram since it has been shown that the discrepancies of the points with respect to the adjusted cylinder respond to a Gaussian distribution. A future approach will automatically detect surface defects in the equipment and, also, the maintenance tasks, almost in real time.

Quantitative results provide numerical information about important parameters as diameters of pipes, shells, distance between equipment and angles, all these obtained from fitting cylinder processing. These parameters are useful for the evaluation of the state of equipment, characterization and temporary monitoring of the state of the machine room of the hospital since the equipment is subject to high pressure and temperature condition. Even slight deformations could be detected if the analyzed parameters are derived for a daily maintenance tasks. The results have been shown to give enough information so that this methodology can be used to evaluate the machine rooms according to the geometrical specifications established in the quality and safety standards and laws for each county whose fulfilment is always of vital importance but, even more critical in the hospital context.

The standards deviations obtained for the diameters are in the order of cm and according to the manufacturer's specifications, in agreement with other current researches [15]. In relative terms, the deviation ranges between 0.50% and 11.21% of the mean diameter value.

Finally, the relative standard deviation for each diameter are correlated using an exponential fit, which yields surprising adjustment results ($R^2 = 0.971$). This data implies that there is an exponential growth of the error with the decrease in diameter and opens new possibilities for the development of prediction algorithms, including approaches based on machine learning strategies which will be addressed in future works.

Although the methodology is suitable for the complete reconstruction of complex machine rooms, the laser systems

have the problem of requiring static objects. So, this technique cannot be correctly applied in facilities with operating workers. This would generate error in the reconstruction and outliers in the scenario. Future lines of work could study the discrimination of moving elements to make the analysis more robust in live environments where people are continuously working. Future lines of work could also study the application of this methodology to work on the three-dimensional model to establish and quantify the required parameters to program concrete changes and maintenance protocols in the machine rooms.

REFERENCES

[1] P. Rodríguez-Gonzálvez *et al.*, "Diachronic reconstruction of lost cultural heritage sites. Study case of the medieval wall of Avila (Spain)," *Int. Arch. Photogramm. Remote Sens. Spatial Inf. Sci.*, vol. XLII-2, pp. 975–981, May 2018, doi: 10.5194/isprs-archives-XLII-2-975-2018.

[2] D. González-Aguilera, S. Del Pozo, G. Lopez, and P. Rodríguez-Gonzálvez, "From point cloud to CAD models: Laser and optics geotechnology for the design of electrical substations," *Opt. Laser Technol.*, vol. 44, no. 5, pp. 1384–1392, Jul. 2012, doi: 10.1016/j.optlastec.2011.12.028.

[3] M. Rodríguez-Martín, P. Rodríguez-Gonzálvez, S. Lagüela, and D. González-Aguilera, "Macro-photogrammetry as a tool for the accurate measurement of three-dimensional misalignment in welding," *Autom. Construct.*, vol. 71, pp. 189–197, Nov. 2016, doi: 10.1016/j.autcon.2016.08.016.

[4] P. Rodríguez-Gonzálvez, M. Rodríguez-Martín, L. F. Ramos, and D. González-Aguilera, "3D reconstruction methods and quality assessment for visual inspection of welds," *Autom. Construct.*, vol. 79, pp. 49–58, Jul. 2017, doi: 10.1016/j.autcon.2017.03.002.

[5] J.-F. Hullo, G. Thibault, C. Boucheny, F. Dory, and A. Mas, "Multi-sensor as-built models of complex industrial architectures," *Remote Sens.*, vol. 7, no. 12, pp. 16339–16362, Dec. 2015, doi: 10.3390/rs71215827.

[6] E. Nocerino, P. Rodríguez-Gonzálvez, and F. Menna, "Introduction to mobile mapping with portable systems," in *Laser Scanning: An Emerging Technology in Structural Engineering*. Boca Raton, FL, USA: CRC Press, to be published.

[7] G. Tucci, D. Visintini, V. Bonora, and E. I. Parisi, "Examination of indoor mobile mapping systems in a diversified internal/external test field," *Appl. Sci.*, vol. 8, no. 3, pp. 401–431, Mar. 2018, doi: 10.3390/app8030401.

[8] S. Nikoohemat, M. Peter, S. O. Elberink, and G. Vosselman, "Exploiting indoor mobile laser scanner trajectories for semantic interpretation of point clouds," *ISPRS Ann. Photogramm. Remote Sens.*, vol. IV-2/W4, no. 8, pp. 355–362, 2017, doi: 10.5194/isprs-annals-IV-2-W4-355-2017.

[9] R. Li, "Mobile mapping: An emerging technology for spatial data acquisition," *Photogramm. Eng. Remote Sens.*, vol. 63, no. 9, pp. 1085–1092, Sep. 1997, doi: 10.1002/9780470979587.ch24.

[10] M. Eyre, A. Wetherelt, and J. Coggan, "Evaluation of automated underground mapping solutions for mining and civil engineering applications," *J. Appl. Remote Sens.*, vol. 10, no. 4, pp. 20–39, Nov. 2016, doi: 10.1117/1.JRS.10.046011.

[11] T. J. B. Dewez, S. Yart, Y. Thuon, P. Pannet, and E. Plat, "Towards cavity-collapse hazard maps with Zeb–Revo handheld laser scanner point clouds," *Photogramm. Rec.*, vol. 32, no. 160, pp. 354–376, Dec. 2017, doi: 10.1111/phor.12223.

[12] E. Nocerino, F. Menna, I. Toschi, D. Morabito, F. Remondino, and P. Rodríguez-Gonzálvez, "Valorisation of history and landscape for promoting the memory of WWI," *J. Cultural Heritage*, vol. 29, pp-113-122, Feb. 2018, doi: 10.1016/j.culher.2017.07.007.

[13] F. Chiabrando, G. Sammartano, and A. Spanò, "A comparison among different optimization levels in 3D multi-sensor models. A test case in emergency context: 2016 Italian earthquake," *Int. Arch. Photogramm. Remote Sens. Spatial Inf. Sci.*, vol. XLII-2/W3, pp. 155–162, Feb. 2017, doi: 10.5194/isprs-archives-XLII-2-W3-155-2017.

[14] C. Cabo, S. Del Pozo, P. Rodríguez-Gonzálvez, C. Ordóñez, and D. González-Aguilera, "Comparing terrestrial laser scanning (TLS) and wearable laser scanning (WLS) for individual tree modeling at plot level," *Remote Sens.*, vol. 10, no. 4, pp. 540–556, Apr. 2018, doi: 10.3390/rs10040540.

[15] E. Nocerino, F. Menna, F. Remondino, I. Toschi, and P. Rodríguez-Gonzálvez, "Investigation of indoor and outdoor performance of two portable mobile mapping systems," *Proc. SPIE*, vol. 10332, p. 103320I, Jun. 2017, doi: 10.1117/12.2270761.

[16] *Machines Rooms and Gas Fired Self Contained Apparatus for Heating or Cooling Generation or Cogeneration*, Standard UNE 60601, AENOR (Spanish Association for Standardisation), 2013.

[17] (2009). *Real Decreto 2060/2008, de 12 de Diciembre, por el que se Aprueba el Reglamento de Equipos a presión y sus Instrucciones técnicas Complementarias, BOE (Official State Gazette of the Government of Spain)*. [Online]. Available: https://boe.es/buscar/doc.php?id=BOE-A-2009-1964

[18] *GeoSlam ZEB-REVO*. Accessed: Jun. 18, 2018. [Online]. Available: https://geoslam.com/wp-content/uploads/2018/04/GeoSLAM-ZEB-REVO-Solution_v9.pdf?x75450

[19] M. Bosse, R. Zlot, and P. Flick, "Zebedee: Design of a spring-mounted 3-D range sensor with application to mobile mapping," *IEEE Trans. Robot.*, vol. 28, no. 5, pp. 1104–1119, Oct. 2012, doi: 10.1109/TRO.2012.2200990.

[20] P. J. Besl and D. N. McKay, "A method for registration of 3-D shapes," *IEEE Trans. Pattern Anal. Mach. Intell.*, vol. 14, no. 2, pp. 239–256, Feb. 1992, doi: 10.1109/34.121791.

[21] *Cloud Compare. GPL Software (Version 2.9.1)*. Accessed: Jun. 18, 2018. [Online]. Available: https://www.danielgm.net/cc/

[22] R. Schnabel, R. Wahl, and R. Klein, "Efficient RANSAC for point-cloud shape detection," *Comput. Graph. Forum*, vol. 26, no. 2, pp. 214–226, May 2007, doi: 10.1111/j.1467-8659.2007.01016.x.

[23] P. Rodríguez-Gonzálvez, J. Garcia-Gago, J. Gomez-Lahoz, and D. González-Aguilera, "Confronting passive and active sensors with non-Gaussian statistics," *Sensors*, vol. 14, no. 8, pp. 13759–13777, Jul. 2014, doi: 10.3390/s140813759.

MANUEL RODRÍGUEZ-MARTÍN was born in Ávila, Spain, in 1988. He received the B.S. degree in industrial engineering from the University of Valladolid, Spain, in 2010, the B.S. degree in mechanical engineering from Nebrija University, Spain, in 2011, the M.S. degree in industrial engineering from the University of Salamanca, Ávila, in 2012, the Ph.D. degree from the University of Salamanca and the University of Vigo in 2015, and the L.L.B. degree from the University of Avila in 2017. He has been an R+D Engineer since 2012, has also been a researcher in the spin-off company ITOS 3D since 2014, and has also been holding a post-doctoral position at the TIDOP Research Group, University of Salamanca, since 2015. He is currently a Professor with the University of Avila and the University of Salamanca, and also a Researcher with the TIDOP Research Group. He has authored over 30 research works related with this topic in international journals, books, and conference proceedings and has worked on different research and technology transfer projects. His research line is based on geotechnologies in the industrial field.

PABLO RODRÍGUEZ-GONZÁLVEZ was born in Oviedo, Spain, in 1983. He received the B.S. degree in surveying engineering from the University of Oviedo in 2004, the M.S. degree in geodesy and cartography from the University of Salamanca, Ávila, Spain, in 2006, and the Ph.D. degree in photogrammetry and computer vision from the University of Salamanca in 2011. From 2013 to 2016, he was a Post-Doctoral Researcher with the University of Salamanca. He is currently an Assistant Professor with the Universidad de León at Ponferrada. He has authored over 70 research articles in international journals and conference proceedings, and 10 inventions. His research lines include photogrammetry 3D reconstruction, accuracy assessment, and radiometric and geometric calibration of the different geomatic sensors. He is also a management committee member of European COST Action CA16219.

DIEGO GONZÁLEZ-AGUILERA was born in Ávila, Spain, in 1976. He received the B.S. degree in surveying engineering and the M.S. degree in geodesy and cartography engineering from the University of Salamanca in 1999 and 2001, respectively. He was a Research Assistant with the Institute of Computer Vision and Robotics, inria, Grenoble, France, where he also performed his Ph.D. research on 3D reconstruction from a single view in 2005. In 2005, he founded the Research Group TIDOP (Geomatic Technologies for the 3D Digitalization and Modeling of Complex Objects), University of Salamanca, where he is currently a Full Professor. He has authored more than 100 research articles in international journals and conference proceedings. Based on his thesis's results, he obtained four international awards of the International Societies of Photogrammetry and Remote Sensing. He is a member of the ISPRS, where he is also serving as a Co-Chair of the Commission II/WG8 and regularly as a program committee member of conferences and a reviewer for related journals.

ERICA NOCERINO received the M.S. degree in navigation sciences from Parthenope University, Italy, in 2006, the Ph.D. degree in aerospatial engineering, naval architecture, and quality control from the University of Naples Federico II, Naples, Italy, in 2015, and the Ph.D. degree in geomatics, navigation, and geodesy from the University of Naples Federico II. From 2012 to 2017, she was a Researcher with the 3DOM Research Group, Bruno Kessler Foundation, Italy. She is currently a Post-Doctoral Researcher with the Laboratoire des Sciences de l'information et des systems, Marseille, France, and also a Researcher with ETH Zürich, Switzerland. She has authored 60 research articles in international journals and conference proceedings. Her research lines include photogrammetry, 3D reconstruction, underwater modeling, and vision metrology. She is a member of ISPRS, where she serves as a Secretary for the Commission II Working Group WG II/7.